

SUPPLEMENTARY INFORMATION: TA-ART-10-2015-008531



Figure S1. Scheme of the equivalent circuit used to fit EIS data.

Sample	R_s (Ωcm^2)	R_1 (Ωcm^2) $\sim 10^5$ Hz. $\sim 10^{-5}$ F cm^{-2} .	R_2 (Ωcm^2) ~ 1000 Hz. $\sim 10^{-4}$ F cm^{-2}	R_3 (Ωcm^2) ~ 50 Hz. $\sim 10^{-2}$ F cm^{-2}	R_4 (Ωcm^2) ~ 10 Hz. $\sim 10^{-1}$ F cm^{-2}	ASR_{cell} (Ωcm^2)
Fuel composition: 3% H ₂ O – 97% H ₂						
PNO1 ini	0.21	0.062	0.40	0.045	0.40	1.12
PNO1 after IV	0.40	0.145	0.50	0.15	0.42	1.61
PNO1 after ~2h	0.56	0.135	0.70	0.17	0.47	2.03
PNO2 ini	0.56	0.009	0.62	0.07	0.26	1.52
PNO2 after IV	0.82	0.10	0.72	0.14	0.30	2.08
PNO2 after ~2h	0.96	0.09	0.77	0.10	0.34	2.26
PNO3 ini	0.10	0.025	0.46	0.065	0.41	1.06
PNO3 after ~100h	0.10	0.025	0.46	0.053	0.40	1.04
Fuel composition: 3% H ₂ O – 97% H ₂						
PNO3 OCV	0.10	0.21	0.22	0.018	0.046	0.59
PNO3 +200mA	0.11	0.03	0.31	0.048	0.044	0.54
PNO3 -200mA	0.10	0.09	0.27	0.037	0.053	0.55

Table S1. Summary of the fitted parameters from EIS analysis.

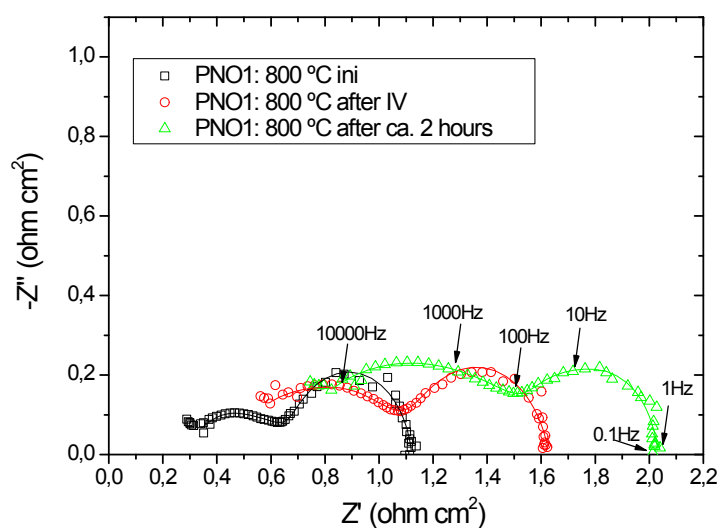


Figure S2. EIS spectra recorded at OCV (800 °C, fuel composition: 3% H₂O – 97% H₂) for the PNO1 cell. Symbols correspond to experimental data and solid lines are the fitted data using the scheme of figure 1.

Based in previous studies for similar cells [28, 31, 36, 44], R1 and R2 were attributed to activation (charge transfer) at the fuel electrode and oxygen electrode, respectively; and R3 and R4 were attributed to gas diffusion (mass transfer) at the oxygen electrode and fuel electrode, respectively. Degradation is clearly observed for the PNO1 cell (figure S2), as there is no interlayer between the YSZ electrolyte and the PNO cathode. As observed from the fitted values (table S1), this degradation is more noticeable from the increase of R_s (ohmic resistance) and R2 (charge transfer at the oxygen electrode), possibly as a consequence of the formation of Pr₂Zr₂O₇ at the interphase induced by the applied current.

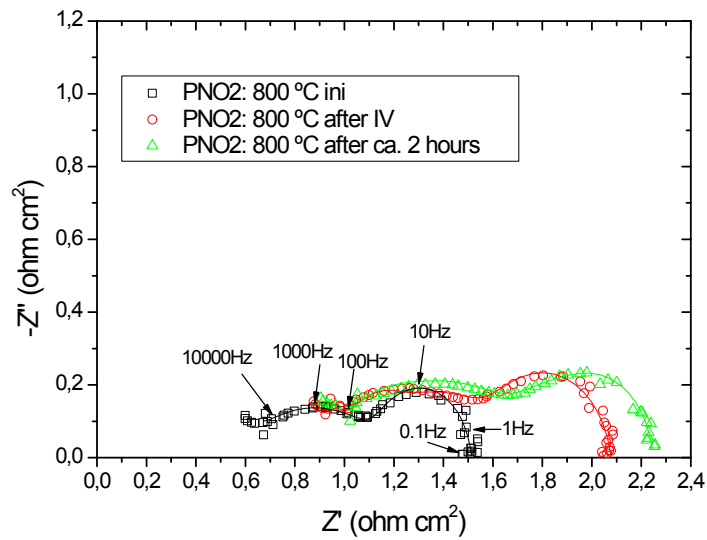


Figure S3. EIS spectra recorded at OCV (800 °C, fuel composition: 3% H₂O – 97% H₂) for the PNO2 cell. Symbols correspond to experimental data and solid lines are the fitted data using the scheme of figure 1.

A similar effect was observed for the PNO2 cell (figure S3). Although in this case there is a GDC barrier layer between the YSZ electrolyte and the PNO oxygen electrode, the densification of this layer seems to be insufficient to avoid the observed degradation. Again, a major increase was observed for both R_s and R_2 components.

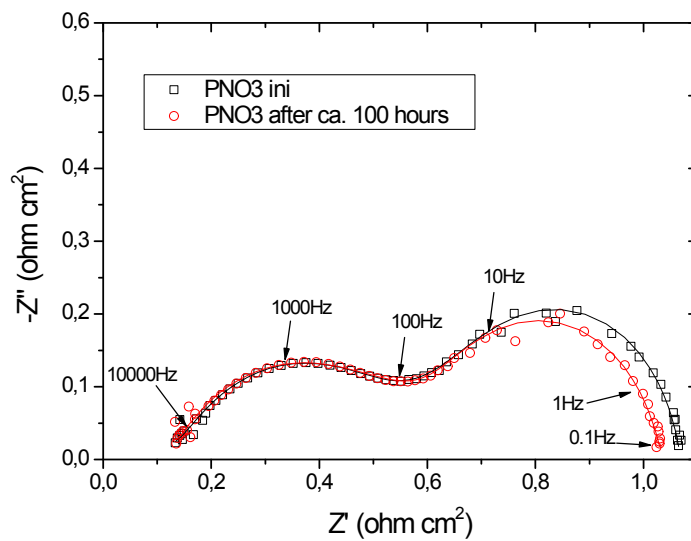


Figure S4. EIS spectra recorded at OCV (800 °C, fuel composition: 3% H₂O – 97% H₂) for the PNO2 cell. Symbols correspond to experimental data and solid lines are the fitted data using the scheme of figure 1.

PNO3 cell showed an excellent stability after about 100 hours under SOFC and SOEC operation conditions (figure S4). In fact, there was a small decrease in the measured EIS spectra, also consistent with the measured *j*-V curves before and after polarization.

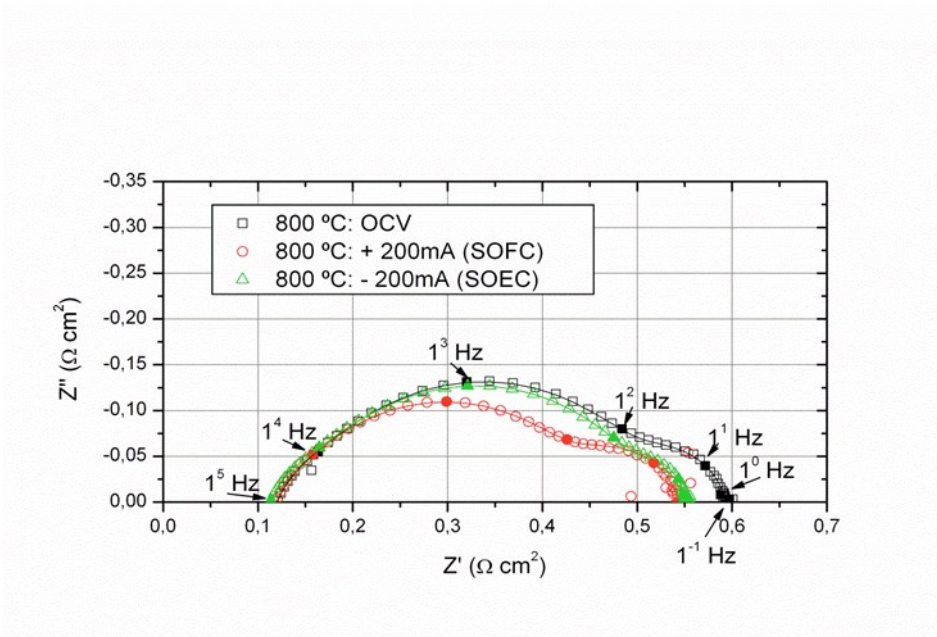


Figure S5. EIS spectra recorded at OCV, +200mA and -200mA (800 °C, fuel composition: 50% H₂O – 50% H₂) for the PNO3 cell. Symbols correspond to experimental data and solid lines are the fitted data using the scheme of figure 1.

EIS experiments under current load using 50% H₂O – 50% H₂ as the fuel gas were also performed (figure S5). Although, the total ASR is rather similar under both anodic and cathodic polarization, we can observe from the values obtained in table S1 that under cathodic polarization (SOEC), R2 and R3 components (attributed to the oxygen electrode), were lowered in comparison with anodic polarization (SOFC). This finding confirms the advantage of the hyperstoichiometry of the PNO phase, making them of particular interest for electrolysis applications.

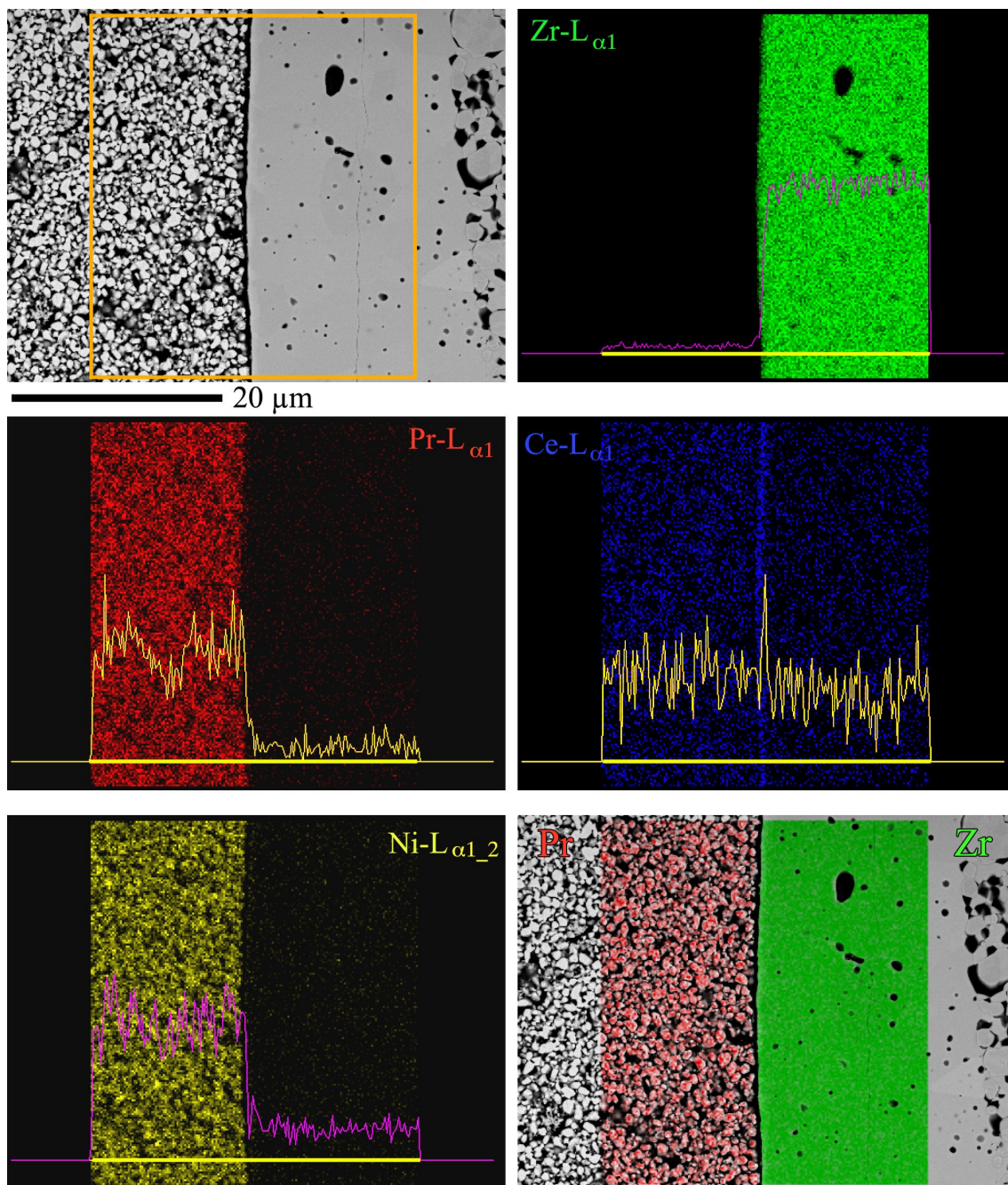


Figure S6. EDS elemental maps at the cathode-electrolyte interface for the PNO3 sample. At the top left of the figure we show the backscattered electron (BSE) image of the analysed area (indicated by the orange rectangle). At the bottom right this image is mixed with the Pr- $L_{\alpha 1}$ (in red) and Zr- $L_{\alpha 1}$ (in green) maps. Each map includes its corresponding line scan obtained along the yellow line. The energy of the electron probe was 10 kV. No reaction between PCGO and YSZ is observed.

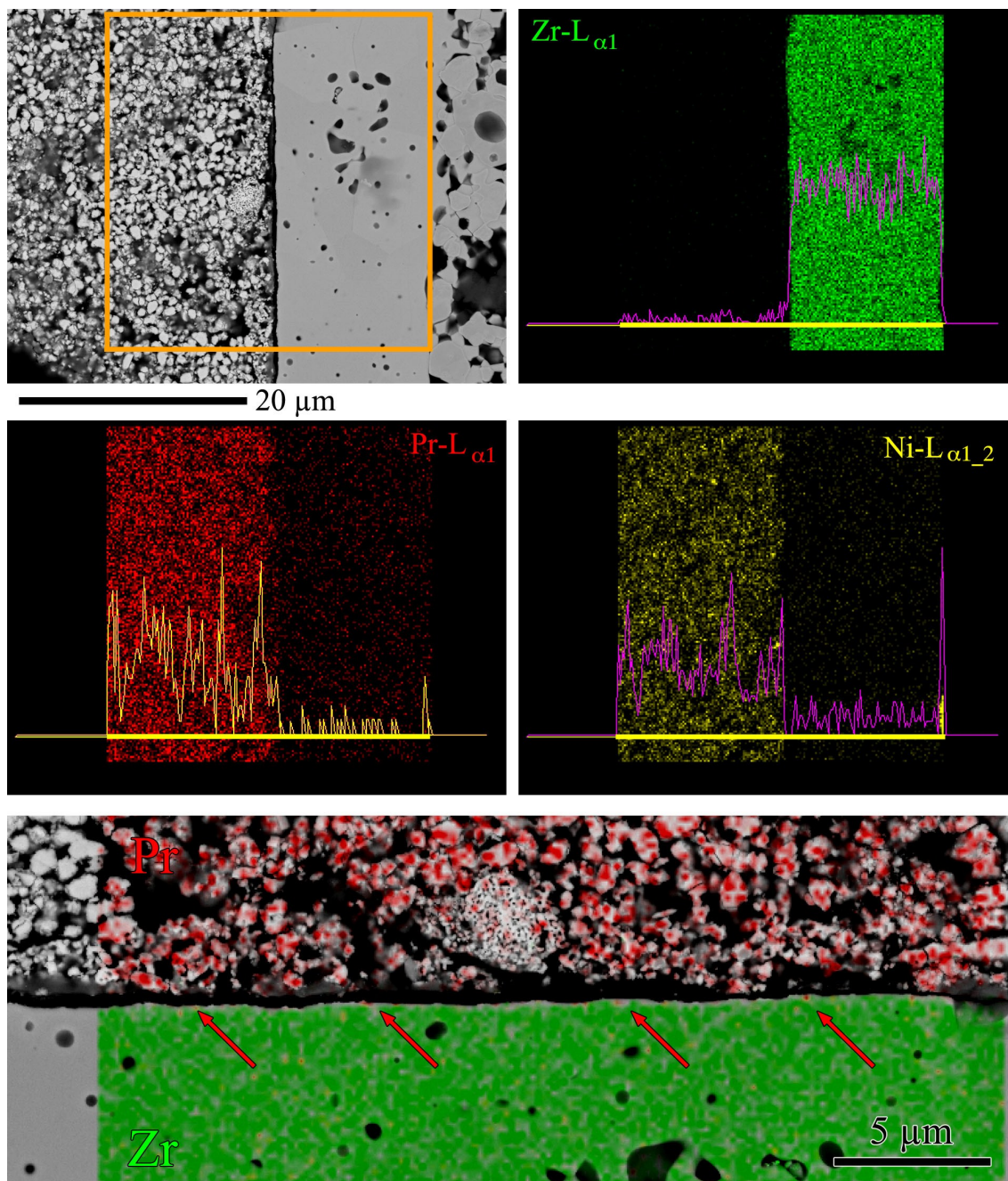


Figure S7. EDS elemental maps at the cathode-electrolyte interface for the PNO1 sample. At the top left of the figure we show the BSE image of the analysed area. Each map includes its corresponding line scan obtained along the yellow line. The energy of the electron probe was 10 kV. At the bottom we shown a zoom of the top-left BSE image (rotated 90°) mixed with the Pr- $L_{\alpha 1}$ (red) and Zr- $L_{\alpha 1}$ (green) maps. The red arrows point out small Pr-rich grains.

Finally, EDS analyses at the interface confirmed that there is no reaction between the PNO oxygen electrode and the YSZ electrolyte for the cells with CGO/PNO composite barrier layer (PNO3). For the cells with no barrier layer (PNO1), 100-250 nm in size Pr-rich grains are detected at the interface. These nanometric grains could correspond to the small amount of $\text{Pr}_2\text{Zr}_2\text{O}_7$ phase detected by XRD experiments.